JBE Journal of Biostatistics and Epidemiology
J Biostat Epidemiol. 2025;11(3): 308-324

ORIGINAL ARTICLE
DOI: *https://doi.org/10.18502/jbe.v11i3.21371/*
*Received **May** 06, 2025; Accepted **June** 24, 2025;*
*Published online **September** 15, 2025.*

Estimation of Volume Under Receiver Operating Characteristic Surface and Asymptotic Variance for Diagnostic Classifier Following Log-Normal Distribution

G **Kumarapandiyan**, T. S. **Sahana***

Department of Statistics, Madras Christian College, University of Madras, Chennai, India.

ABSTRACT

Introduction: Clinical diagnosis highlights the essential need to assess biomarker performance for effective disease screening and diagnosis. The Receiver Operating Characteristic (ROC) curve serves as a fundamental tool for assessing and interpreting biomarker effectiveness. Numerous models and techniques have been developed to analyze biomarkers in binary classification settings (Non-Diseased vs. Diseased). This research article seeks to expand the binary classification framework to a three-class scenario, incorporating Diseased, Suspicious, and Non-Diseased categories under a Log-Normal distribution.

Methods: It introduces a three-class Log-Normal ROC model based on a Parametric approach, deriving metrics such as Volume Under the ROC Surface (VUS) and Asymptotic Variance, as well as an alternative Non-Parametric approach. The model was validated using simulated data generated for the underlying distribution, and a real-life dataset was used to fit the VUS and ROC curves.

Results: The simulation study was conducted using four sets with varying parameters. In the fourth set, the Non-Parametric VUS (0.9966) exceeded the Parametric VUS (0.8058), though the difference was smaller compared to the other sets. The low Standard Error (SE) (0.0472) across all sets indicates high precision in the estimates. Additionally, for the real-life (The multiple sclerosis (ms) disease) dataset the VUS value is 0.6782 which gives moderate fit of the model.

Conclusion: In this study, we derived the asymptotic variance and VUS for the Log-Normal distribution using simulated data with varying parameters. The analysis compares diagnostic performance across parameter sets, highlighting the superiority of Non-Parametric VUS over Parametric VUS. Set 4 demonstrated the highest reliability with the lowest standard error (SE = 0.0472). The real-life MS dataset provided a moderate fit to the proposed model.

Key words: Biomarker; Gold standard; Three class classification; Receiver operating characteristics; Volume under the ROC surface and asymptotic variance

*Corresponding Author:
sahanaram2926@gmail.com

INTRODUCTION

Biomarkers are quantifiable indicators of a biological state or condition, used to diagnose and monitor diseases by providing objective data to guide clinical decision-making. The gold standard test, recognized for its precision, serves as the reference point for assessing the effectiveness of new diagnostic tools, including biomarkers.[1,2] The ROC curve plays a key role in this evaluation process, illustrating and quantifying the ability of a biomarker or test to differentiate between two separate conditions or groups (Non-diseased and Diseased).[3]

In this article, we further extend the two-way classification to a three-class approach (Diseased, Suspicious, and Non-Diseased). However, there is a scarcity of parametric methods designed to evaluate a biomarker that categorizes an individual into three or multiple classes. Applying ROC analysis to multi-class problems involves assessing the trade-offs in misclassification rates between the three classes.[2]

1.1 Parametric Approach to Two-Class and Three-Class ROC Analysis

a. The evaluation process of two class problem is listed as follows:

The threshold 't' in equation (1) is determined initially by combining the Non-Diseased and Diseased sets into a single set, say 'B_i'. Then, a random threshold value 't' is selected within the range between the maximum and minimum values of 'B_i' for each value in 'B_i'.

$$P=\begin{cases} B_i \leq t & Non-Diseased \\ B_i > t & Diseased \end{cases} \quad (1)$$

where 't' is the threshold and 'P' is the probability of classification

Now, we have two classification criteria, i.e., one is the gold standard and the other is defined by equation (1). With these two criteria, we obtain the following probabilities:

True Positive Rate (TPR)

It is the proportion of diseased detected by the test to the total number of diseased people. It is also called Sensitivity.

True Negative Rate (TNR)

It is the proportion of non-diseased subjects identified correctly by the test. It is sometimes referred to as Specificity.

False Positive Rate (FPR)

It is the proportion of non-diseased subjects identified as diseased by the test. It is sometimes referred to as 1- Specificity.

False Negative Rate (FNR)

It is the proportion of diseased subjects identified as non-diseased by the test. It is also referred to as 1- Sensitivity.

Each threshold 't' leads to a 2×2 contingency table given in Table 1 containing the true and false classification probabilities. The chance line in a two-class ROC curve is the diagonal from (0,0) to (1,1), symbolizing a model with no ability to distinguish between classes. It reflects random prediction, where the True Positive Rate matches the False Positive Rate.

Table 1. Performance evaluation of a two-class classification model using a 2×2 confusion matrix

Actual Status (Gold Standard)	Result of the classifier (Diagnostic Marker)	
	Diseased	Non-Diseased
Diseased	TPR=P(Y>t)	FNR=P(Y≤t)
Non-Diseased	FPR=P(X>t)	TNR=P(X≤t)

TPR, True Positive Rate; FNR, False Negative Rate; FPR, False Positive Rate; TNR, True Negative Rate

A two-class ROC curve can be constructed by graphing FPR against TPR, where FPR is on the horizontal axis and TPR is on the vertical axis. The primary goal is to reduce misclassifications, encompassing both FPR and FNR. Sensitivity and Specificity of the test are identified at probability values where True Classification (TC) rates are notably high and False Classification (FC) rates are notably low. The Area Under the ROC Curve (AUC) serves as a summary measure of a diagnostic test's accuracy. It represents the test's overall ability to distinguish between all possible thresholds. A higher AUC value, approaching 1, signifies superior discriminative capacity, indicating that the test or biomarker can effectively differentiate between Non-Diseased and Diseased.[4]

Suppose X and Y represent two random variables indicating biomarker values from populations of Non-diseased and Diseased individuals. Assume that X and Y follow continuous distributions characterized by F(x) and G(y) as their respective cumulative distribution functions. The representation of the ROC model for plotting ROC curves is structured as follows.[5, 3]

$$ROC(t) = \bar{G}_Y \circ \bar{F}_X^{-1}(t);\ 0 < \bar{F}_X(t) < 1$$

$$\mathrm{AUC} = \mathrm{P}(\mathrm{Y} > \mathrm{X}) = \int_0^1 ROC(t)\ \mathrm{dt} = \int_0^1 \bar{G}_Y \circ \bar{F}_X^{-1}(t)\ \mathrm{dt} \quad (2)$$

where,

$$\bar{F}_X(t) = P(X > t)$$

$$\bar{F}_X(t) = \int_t^\infty f(x)dx \quad (3)$$

$$\bar{G}_Y(t) = P(Y > t)$$

$$\bar{G}_Y(t) = \int_t^\infty g(y)dy \quad (4)$$

Additionally, the Bi-Normal model tends to generate a degenerated ROC curve (crossing below the chance line, connecting (0,0) and (1,1)) when dealing with small sample sizes. In such cases, the Bi-Lognormal ROC model proves to be highly beneficial. The Lognormal distribution is particularly useful for datasets that exhibit positive skewness. The Bi-Lognormal ROC curve exhibits an asymmetry property.[6,7]

b. The evaluation process of three-class problem (Parametric Case)

A three-class ROC surface can be used in medical diagnosis to assess the effectiveness of a diagnostic test or biomarker that divides the subject into three groups: Diseased, Suspicious, and Non-Diseased using two thresholds t_1 and t_2. A three-dimensional extension of the AUC that offers a more thorough evaluation of the effectiveness of the biomarker is the VUS.[8] Here the ROC surface is fitted using the true classification rates, i.e. (TC_1, TC_2, and TC_3).[9]

Let X, Y, and Z be the random variables representing the biomarker values of Diseased, Suspicious, and Non-Diseased groups respectively. These variables assume continuous Log-Normal distribution, i.e., $X_i \sim F_X(.)$; i = 1, 2,…, m, $Y_j \sim F_Y(.)$; j = 1, 2,…, n and $Z_k \sim F_Z(.)$; k = 1, 2,..., p. As in the two-class approach, combine the biomarker values of all the three groups together to form a single set, say 'B_i' (i = 1, 2,…, N; where N= m + n + p; m, n and p be the number of observations from Diseased, Suspicious, and Non-diseased groups, respectively). For each set of two ordered thresholds t_1 and t_2 ($t_1 < t_2$), assign a probability score for each class, and they are defined as follows:

$P(B_i > t_2)$: The probability that the data point B_i belongs to a Diseased group
$P(t_1 < B_i \leq t_2)$: The probability that the data point B_i belongs to a Suspicious group
$P(B_i \leq t_1)$: The probability that the data point B_i belongs to a Non-Diseased group
The 3×3 contingency table for thresholds t_1 and t_2 is shown in table 2.

Table 2. Performance evaluation of a three-class classification model using a 3×3 confusion matrix

Results from the Gold Standard	Results from the Diagnostic test		
	Non- Diseased	Suspicious	Diseased
Non-Diseased	$TC_1 = P(Z \leq t_1)$	$FC_1 = P(t_1 < Z \leq t_2)$	$FC_2 = P(Z > t_2)$
Suspicious	$FC_3 = P(Y \leq t_1)$	$TC_2 = P(t_1 < Y \leq t_2)$	$FC_4 = P(Y > t_2)$
Diseased	$FC_5 = P(X \leq t_1)$	$FC_6 = P(t_1 < X \leq t_2)$	$TC_3 = P(X > t_2)$

TC, True Classification; FC, False Classification

If TC and FC are the correct and false classifications, respectively, then TC_1 is the probability of correctly identifying non-diseased individuals, TC_2 is the probability of correctly identifying suspicious individuals, and TC_3 is the probability of correctly identifying diseased individuals. The remaining six misclassifications that occur during the classification procedure using t_1 and t_2 are: FC_1 (Non-diseased subjects are misidentified as Suspicious), FC_2 (Non-diseased subjects are identified as Diseased), FC_3 (Suspicious are incorrectly identified as Non-diseased), FC_4 (Suspicious are misidentified as Diseased), FC_5 (Diseased are misidentified as Non-diseased), and FC_6 (Diseased are misidentified as

Suspicious). The general ROC surface model is given by

$$P(Z \leq t_1) = F_Z(t_1) \tag{5}$$

$$(t_1 < Y \leq t_2) = F_Y(t_2) - F_Y(t_1) \tag{6}$$

$$\mathrm{P}(\mathrm{X} > t_2) = 1 - F_X(t_2) \tag{7}$$

Substitute equations (5) and (7) in 6, We get,

$$ROC(t_1, t_2) = F_Y(F_Z^{-1}(t_2)) - F_Y(F_Z^{-1}(t_1)); -\infty < t_1, t_2 < \infty \tag{8}$$

A typical ROC surface plot will look like the one presented in Figure 1. In this plot, the x-axis represents TC_1, the y-axis represents TC_2, and the z-axis represents TC_3.[10]

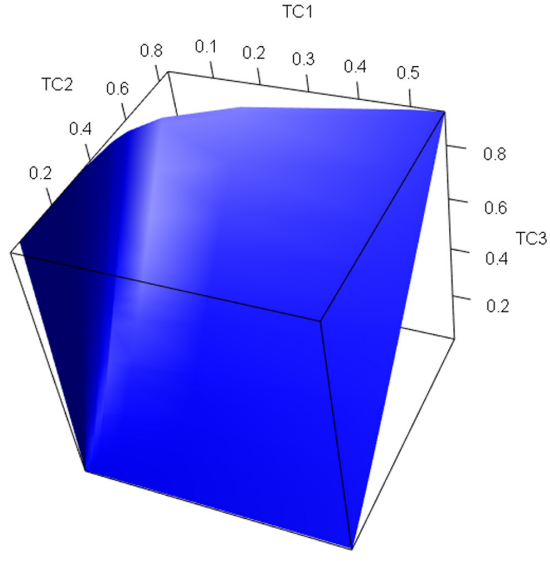

Figure 1. The general ROC plot
ROC, Receiver operating characteristics; TC, True Classification

Let us assume that biomarker values from the three groups follow Log-Normal distribution individually, i.e., $X \sim F_x(X)$, $Y \sim F_y(Y)$ and $Z \sim F_z(Z)$ where X, Y and Z are mutually independent. The Cumulative Distribution Function (CDF) is given by:

$$\begin{aligned} F_x(X) &= \Phi\left(\frac{\log(X) - \mu_X}{\sigma_X}\right) \\ F_y(Y) &= \Phi\left(\frac{\log(Y) - \mu_Y}{\sigma_Y}\right) \\ F_z(Z) &= \Phi\left(\frac{\log(Z) - \mu_z}{\sigma_z}\right) \end{aligned} \tag{9}$$

The ROC surface can be plotted by the following coordinates for the different values of the thresholds t_1 and t_2.

$$\left(\Phi\frac{\frac{t_1-\mu_X}{\sigma_X}}{\sigma_X}\right)-\left(\Phi\frac{\frac{t_1-\mu_Y}{\sigma_Y}}{\sigma_Y}\right)\left(\Phi\frac{\frac{t_2-\mu_Y}{\sigma_Y}}{\sigma_Y}\right)-\left(\Phi\frac{\frac{t_2-\mu_Z}{\sigma_Z}}{\sigma_Z}\right) \quad (10)$$

1.2 Non - Parametric Approach to Two-Class and Three-Class ROC Analysis

a. The Evaluation process of two-class ROC (Non-Parametric Case)

Let x_i represent the biomarker value of Non-Diseased subjects and y_j represent the biomarker value of Diseased subjects. For each pair of [x_i, y_j], we can have indicator function[11]

$$I(x_i,y_j)=\begin{cases}1 & if\ y_j>x_i\\ \frac{1}{2} & if\ y_j=x_i\\ 0 & if\ y_j<x_i\end{cases} \quad (11)$$

where i = 1,2,3, ……m and j = 1,2,3,……n
The probability of AUS is given by

$$\text{AUS}=\text{P(Y}>\text{X)}=\sum_{i=1}^{m}\sum_{j=1}^{n}\frac{(x_i,y_j)}{mn} \quad (12)$$

where m and n are the sample sizes of Non-Diseased and Diseased classes.

b. The Evaluation process of three-class ROC (Non-Parametric Case)

Let X_i,Y_j, Z_k represent the biomarker values of Non-Diseased, Suspicious and Diseased groups and the Non-Parametric expression of VUS is given by[12, 2]

$$VUS=P\ (X>Y\ >\ Z)=\sum_{i=1}^{m}\sum_{j=1}^{n}\sum_{k=1}^{p}\frac{I(X_i,\ Y_j,Z_k)}{mnp} \quad (13)$$

where,

$$I(X_i,Y_j,Z_k)=\begin{cases}1 & if\ Z<Y<X\\ 0.5 & if\ Z=Y<X\\ 0.5 & if\ \text{Z}<\text{Y}=\text{X}\\ 0 & if\ \text{Z}>\text{Y}>\text{X}\\ \frac{1}{6} & if\ (Z=Y=X)\end{cases} \quad (14)$$

where m, n and p are the sample size of the variables Non - Diseased, Suspicious and Diseased $I(X_i, Y_j, Z_k)$ is indicator function. This indicator function assigns different values based on the relative order of $I(X_i, Y_j, Z_k)$. By summing these indicator values over all possible combinations of i, j and k, then dividing by the product of the sample sizes m, n, and p, we obtain the non-parametric estimate of the VUS. The VUS scale spans from 0 to 1. VUS score of 1 signifies an ideal model capable of achieving flawless classification across all classes.[12, 13]

METHODS

Derivation of Tri-Class Log-Normal VUS:

In this paper, the Tri-Class Log-Normal ROC surface has been developed for a continuous biomarker, extending the Tri-Class Log-Normal ROC curve [14]. Let $F_x(X)$, $F_y(Y)$ and $F_z(Z)$ be the CDF of Tri-Class Log-Normal ROC, and the VUS is calculated by solving the below integral.

$$\text{VUS} = V(X - Y - Z) = \text{Var}(X) + \text{Var}(Y) + V(Z)$$

$$VUS = \sigma_x^2 + \sigma_y^2 + \sigma_z^2 \tag{15}$$

$$\text{Z-Y-X} \sim N((\mu_x - \mu_y - \mu_z),(\sigma_x^2 + \sigma_y^2 + \sigma_z^2)) \tag{16}$$

After solving the equation (15) and (16), the result is obtained as follows:

$$\text{VUS} = \delta = \frac{(\mu_x - \mu_y - \mu_z)}{\sqrt{\sigma_x^2 + \sigma_y^2 + \sigma_z^2}} \tag{17}$$

The equation (17) explains the parametric VUS of the Tri-Class Log-Normal distribution. Nevertheless, software like Mathematica can facilitate the computation of intricate integrations to derive this metric.[15]

Asymptotic Variance of VUS for Tri-Class Log-Normal Distribution

The Maximum Likelihood Estimator (MLE) of δ is given by

$$\hat{\delta} = \frac{(\mu_x - \mu_y - \mu_z)}{\sqrt{\sigma_x^2 + \sigma_y^2 + \sigma_z^2}} \tag{18}$$

Since $\Phi(\hat{\delta})$ is a monotonically increasing function of $\hat{\delta}$, calculating the variance and standard error of $\hat{\delta}$ is sufficient to determining the confidence interval for AUC. Since δ is a function of parameters $\theta = (\mu_x, \mu_y, \mu_z, \sigma_x^2 + \sigma_y^2 + \sigma_z^2)$ we will adopt the delta method to find the approximate variance and standard error of $\hat{\delta}$.[16]

$$\begin{aligned} V(\hat{\delta}) = {} & \left(\frac{\partial\delta}{\partial\mu_z}\right)^2 V(\hat{\mu}_z) + \left(\frac{\partial\delta}{\partial\mu_y}\right)^2 V(\hat{\mu}_y) + \left(\frac{\partial\delta}{\partial\mu_x}\right)^2 V(\hat{\mu}_x) + \left(\frac{\partial\delta}{\partial\sigma_y^2}\right)^2 V(\hat{\sigma}_y^2) \\ & + \left(\frac{\partial\delta}{\partial\sigma_x^2}\right)^2 V(\hat{\sigma}_x^2) + \left(\frac{\partial\delta}{\partial\sigma_z^2}\right)^2 V(\hat{\sigma}_z^2) + 2(\hat{\mu}_y, \hat{\mu}_x) + 2(\hat{\mu}_x, \hat{\mu}_z) + 2(\hat{\mu}_y, \hat{\mu}_z) \\ & + 2(\sigma_x^2, \hat{\mu}_x) + 2(\sigma_y^2, \hat{\mu}_y) + 2(\sigma_z^2, \hat{\mu}_z) + 2(\sigma_x^2, \sigma_y^2) + 2(\sigma_y^2, \sigma_z^2) \\ & + 2(\sigma_z^2, \sigma_x^2) \end{aligned} \tag{19}$$

$$\frac{\partial \delta}{\partial \mu_x} = \frac{-1}{\sqrt{\sigma_x^2 + \sigma_y^2 + \sigma_z^2}}$$
$$\frac{\partial \delta}{\partial \mu_y} = \frac{-1}{\sqrt{\sigma_x^2 + \sigma_y^2 + \sigma_z^2}} \quad (20)$$
$$\frac{\partial \delta}{\partial \mu_z} = \frac{-1}{\sqrt{\sigma_x^2 + \sigma_y^2 + \sigma_z^2}}$$

$$\frac{\partial \delta}{\partial \sigma_x^2} = \left(\frac{-(\mu_z - \mu_y - \mu_x)}{2(\sigma_x^2 + \sigma_y^2 + \sigma_z^2)^{\frac{3}{2}}} \right)^2$$
$$\frac{\partial \delta}{\partial \sigma_y^2} = \left(\frac{-(\mu_z - \mu_y - \mu_x)}{2(\sigma_x^2 + \sigma_y^2 + \sigma_z^2)^{\frac{3}{2}}} \right)^2 \quad (21)$$
$$\frac{\partial \delta}{\partial \sigma_z^2} = \left(\frac{-(\mu_z - \mu_y - \mu_x)}{2(\sigma_x^2 + \sigma_y^2 + \sigma_z^2)^{\frac{3}{2}}} \right)^2$$

All the 9 pairs of co-variance becomes 0 and the diagonal elements are $\frac{\sigma_x^2}{m}, \frac{\sigma_y^2}{n}, \frac{\sigma_z^2}{p}$ By substituting equation (20) and (21) in (19) we get,

$$\frac{-1}{\sqrt{\sigma_x^2 + \sigma_y^2 + \sigma_z^2}} \frac{\sigma_x^2}{m} + \frac{-1}{\sqrt{\sigma_x^2 + \sigma_y^2 + \sigma_z^2}} \frac{\sigma_y^2}{n} + \frac{-1}{\sqrt{\sigma_x^2 + \sigma_y^2 + \sigma_z^2}} \frac{\sigma_z^2}{p}$$
$$+ \left(\frac{-(\mu_z - \mu_y - \mu_x)}{2(\sigma_x^2 + \sigma_y^2 + \sigma_z^2)^{\frac{3}{2}}} \right)^2 \frac{2\sigma_x^4}{m-1} + \left(\frac{-(\mu_z - \mu_y - \mu_x)}{2(\sigma_x^2 + \sigma_y^2 + \sigma_z^2)^{\frac{3}{2}}} \right)^2 \frac{2\sigma_y^4}{n-1} \quad (22)$$
$$+ \left(\frac{-(\mu_z - \mu_y - \mu_x)}{2(\sigma_x^2 + \sigma_y^2 + \sigma_z^2)^{\frac{3}{2}}} \right)^2 \frac{2\sigma_z^4}{p-1}$$

Higher-order effects, involving both variances and differences in means, are also included to improve the accuracy of the variance estimate, especially when sample sizes are not large. This type of expression is typically encountered when applying the delta method to approximate the variance of a nonlinear function of random variables.[14]

RESULTS

This section provides a comparative analysis of the simulation studies carried out under the log-normal ROC and normal ROC models. The real life dataset multiple sclerosis disease dataset are employed to compare the Tri-Class Log-Normal and normal distribution ROC and its VUS. The investigation focused on the Tri-Class Log-Normal distribution ROC model through simulated studies. Samples of identical sizes (30, 30, 30) were generated using the Log-Normal distribution with diverse parametric values μ_X={0.6,0.5,0.75,0.6} , μ_Y={1.1,1.2,1.1,1.3} and μ_z={1.9,1.9,1.85,2.0}

and σ_X={0.25,0.2,0.15,0.2},σ_Y={0.35,0.3,0.25,0.25} and σ_Z={0.5,0.4,0.2,0.3}. The multiple sclerosis (ms) disease that is downloaded from data.gov and here we categorized the data into three groups: Cerebrospinal Fluid, Immunoglobulin G, and Albumin and the VUS is calculated for the same. Table 3 explains the simulation studies of the samples generated, and furthermore, the analysis involves fitting a density plot for the Log-Normal distribution. Table 4 explains the Comparison of Log-Normal and Normal ROC model for Real-Life Dataset The density plot is shown in Figure 2, 3, 4 and 5.

Table 3. Comparison of Simulation Studies Presenting ROC Surfaces for Various Parametric Values under Log-Normal and Normal Distributions

Set of parameters	Parameters	Estimated means	VUS Parametric and SE (Log-Normal)	VUS Parametric and SE (Normal)	VUS Non-Parametric
1	μ_x= 0.6, σ_x=0.25 μ_y=1.1, σ_y=0.35 μ_z=1.9, σ_z=0.5	1.8799 3.1939 7.5761	0.5921 (0.063)	0.004 (0.5849)	0.9044
2	μ_x=0.5, σ_x=0.2 μ_y=1.2, σ_y=0.3 μ_z=1.9, σ_z=0.4	1.6820 3.4729 7.2427	0.6489 (0.0539)	0.0395 (0.4836)	0.9144
3	μ_x= 0.75, σ_x=0.15 μ_y=1.1, σ_y=0.25 μ_z=1.85, σ_z=0.2	2.1400 3.0995 6.4883	0.7985 (0.0502)	0.2386 (0.2183)	0.9156
4	μ_x= 0.6, σ_x=0.2 μ_y=1.3, σ_y=0.25 μ_z=2.0, σ_z=0.3	1.8589 3.7858 7.7292	0.8058(0.0472)	0.3486 (0.1148)	0.9966

TC, True Classification; FC, False Classification

Table 4. Comparison of Log-Normal and Normal ROC model for Real-Life Dataset

VUS for Log normal	SE for Log normal	VUS for Normal	SE for Normal
0.6782	0.0985	0.3623	0.8345

VUS, Volume Under; SE, Standard Error

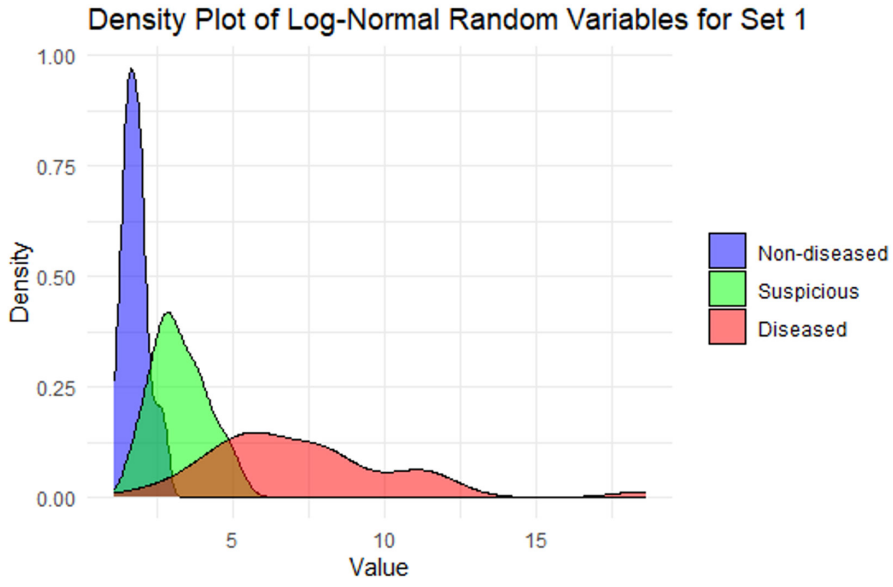

Figure 2. Density Plot for the SET 1 parameters

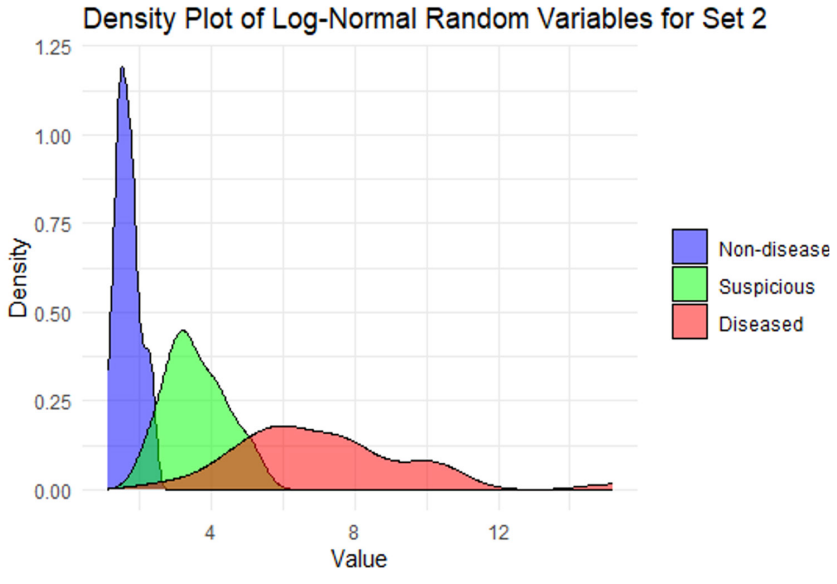

Figure 3. Density Plot for the SET 2 parameters

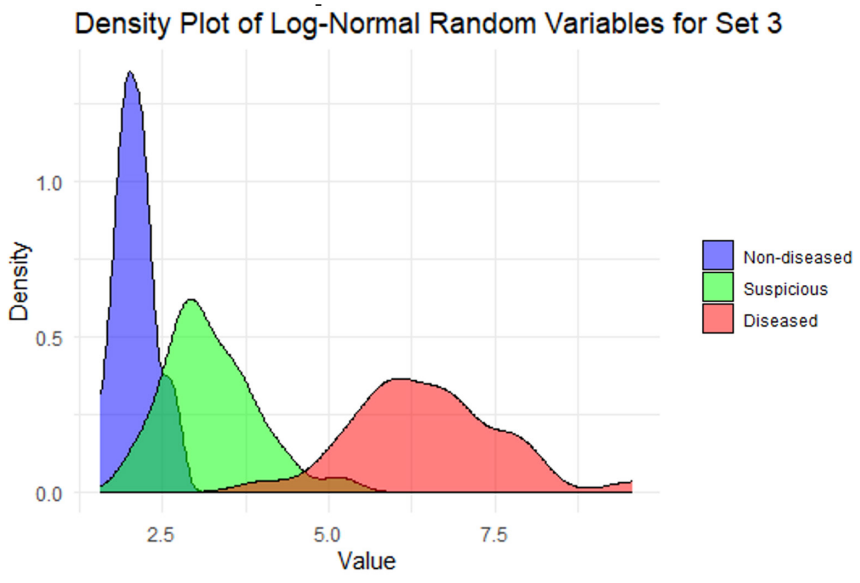

Figure 4. Density Plot for the SET 3 Parameters

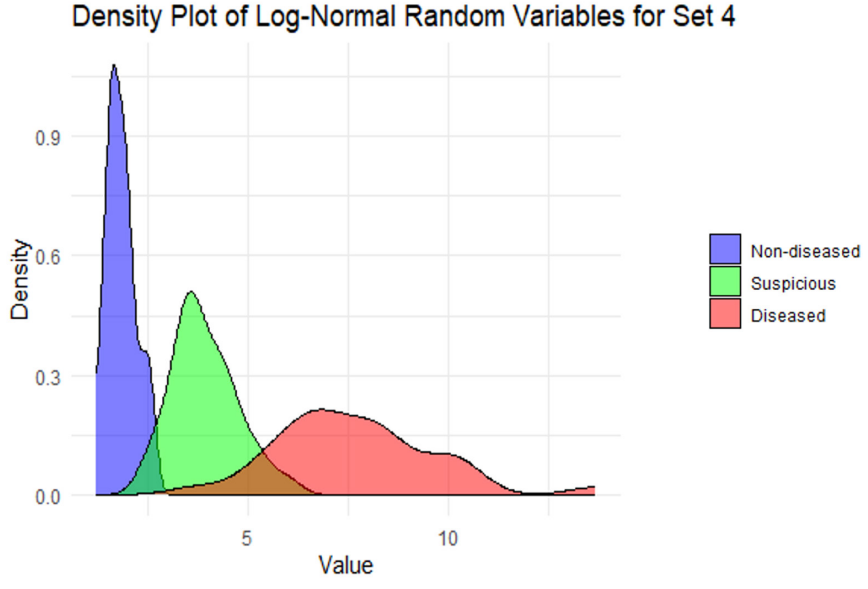

Figure 5. Density Plot for the SET 4 Parameters

a. Parametric ROC curve

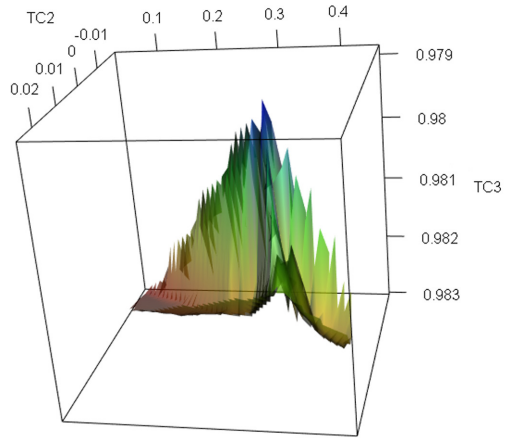

Figure 6. ROC Plot for the SET 1 Parameters

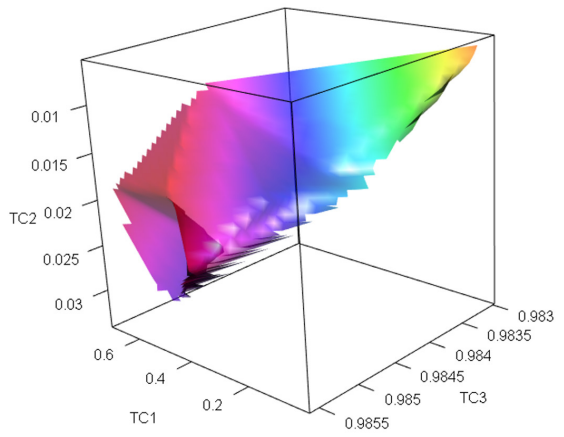

Figure 7. ROC Plot for the SET 2 Parameters

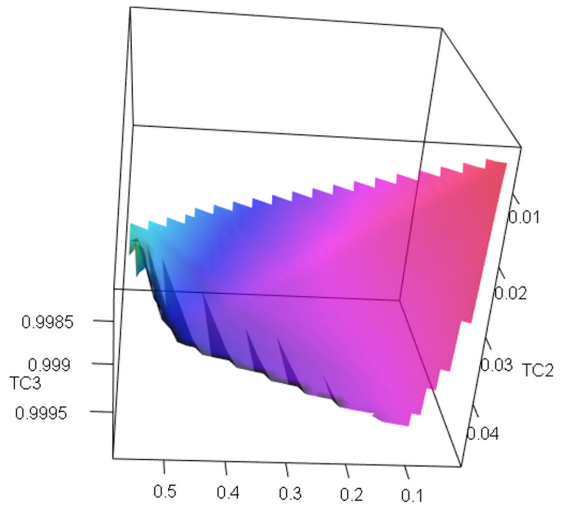

Figure 8. ROC Plot for the SET 3 Parameters

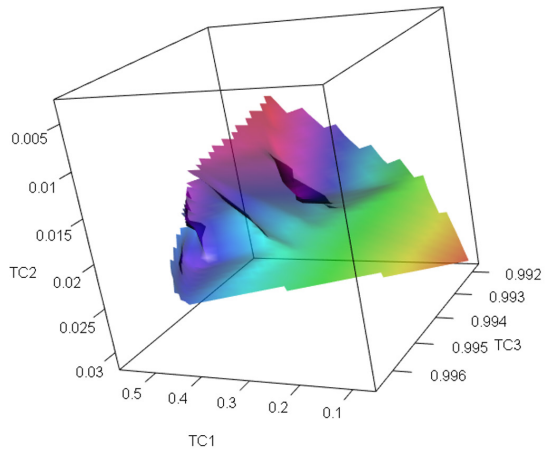

Figure 9. ROC Plot for the SET 4 Parameters

b. Non-Parametric ROC curve

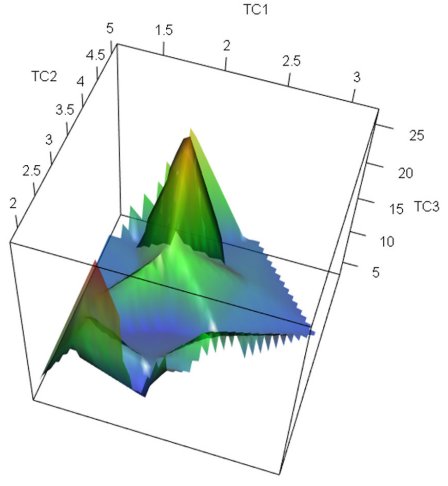

Figure 10. Non-Parametric ROC plot for the SET 1 parameters

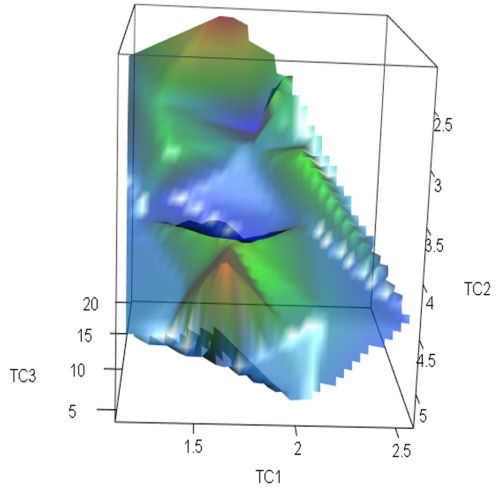

Figure 11. Non-Parametric ROC plot for the SET 2 parameters

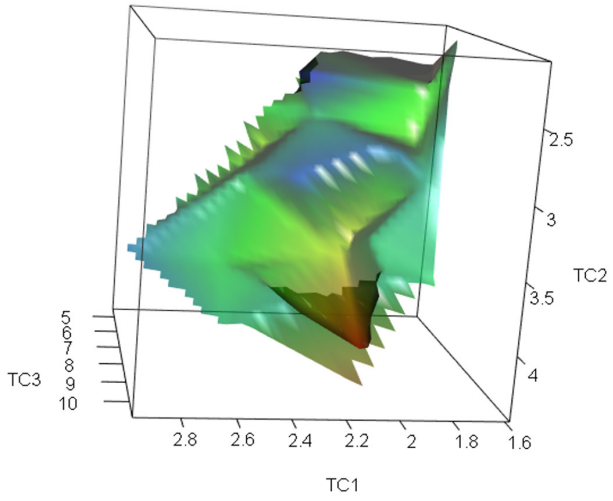

Figure 12. Non-Parametric ROC plot for the SET 3 parameters

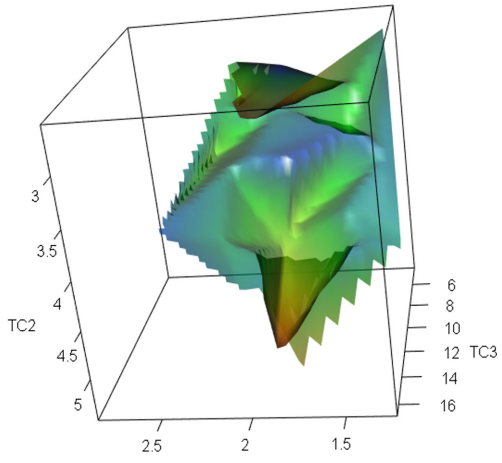

Figure 13. Non-Parametric ROC plot for the SET 4 parameters

c. For the Real-Life Dataset

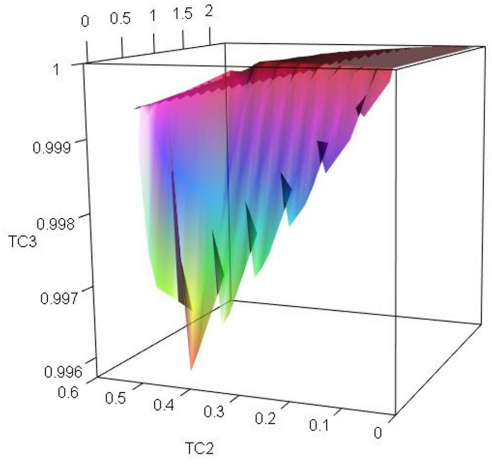

Figure 14. ROC Graph for the Real-Life Dataset

DISCUSSION

The analysis across four sets of parameters reveals important insights into the diagnostic performance of Log-Normal, Normal, and Non-Parametric ROC approaches based on the VUS. Among the two parametric methods, the Log-Normal ROC model consistently outperforms the Normal ROC model, exhibiting higher VUS values with considerably lower standard errors. This demonstrates that the Log-Normal ROC is better suited for modeling the diagnostic ability of the data, which often exhibit positive skewness. For instance, in Set 4, the Log-Normal model achieved a VUS of 0.8058 (SE = 0.0472), compared to 0.3486 (SE = 0.1148) for the normal ROC model. Such results affirm that the Log-Normal ROC model not only delivers better discriminatory power but also offers more precision and stability in its estimates, making it a reliable parametric choice for multi-class diagnostic modeling.

Among all tested parameter sets, the Non-Parametric method demonstrated superior performance, achieving an almost ideal VUS value of 0.9966 in set 4. Since non-parametric ROC model do not rely on assumptions about the underlying data distribution, they are more effective with small and well-structured datasets. On other hand, they underperform when the dataset is large and has complex settings. In contrast, the Log-Normal ROC model offers a favorable balance between model interpretability and classification accuracy. It provides robust performance, even with moderate sample sizes, and retains the advantages of a parametric framework, such as ease of implementation, computational efficiency, and theoretical tractability. Although the non-parametric method can serve as a performance benchmark, the Log-Normal model proves to be a practical and reliable option for diagnostic tasks involving skewed data.

The VUS and SE values of real life dataset for both the Log-Normal and Normal models reveal significant differences in performance. The VUS for the Log-Normal model is 0.6782 with a relatively small SE of 0.0985, indicating that the diagnostic classifier exhibits moderate discriminatory power and that this estimate is stable and reliable. In contrast, the Normal model yields a VUS of only 0.3623, which is well below the 0.5 threshold suggesting the classifier performs worse than random chance under the normality assumption. Furthermore, the associated SE of 0.8345 is very high, pointing to substantial variability and unreliability in the estimate. These results strongly support the suitability of the Log-Normal ROC model over the Normal ROC model, as it provides a more accurate and dependable representation of the data for evaluating diagnostic classifier performance.

Figure 6,7,8 and 9 depict the parametric ROC for the Tri-Class Log-Normal distribution. A greater VUS often signifies superior model performance. This suggests that the model exhibits strong performance across diverse threshold settings and potentially across varying values of the third dimension. ROC curves are instrumental in monitoring how performance metrics shift due to changes in thresholds or other parameters affecting the model.

Figures 10 to 13 depict the Non-Parametric ROC plots for various parameter sets, demonstrating that the Non-Parametric approach consistently yields higher VUS values than the Parametric method. Looking at the provided figures, the increase in the curve's area aligns with the parameter's variation,

indicating that as the parameter difference grows, the model's fit improves. In essence, a larger area under the ROC curve reflects enhanced discriminative ability, implying that the model performs better in distinguishing between classes or conditions as the parameter differences increase. The ROC curve in figure 14 illustrates a moderate level of separation between the TC_1,TC_2 and TC_3 across various thresholds, reflecting moderate discriminatory power.

CONCLUSION

In this article, we have obtained the asymptotic variance and VUS for the Tri-class Log-Normal distribution and assessed the performance of the proposed model with the simulated and real-life dataset. To conclude, the analysis across the four parameter sets clearly demonstrates the superior diagnostic performance of the tri-class log-Normal ROC model compared to the normal ROC model, while also shedding light on the strengths and limitations of parametric versus non-parametric approaches. The log-Normal ROC model consistently yields higher VUS values accompanied by lower standard errors, reinforcing its effectiveness in capturing the characteristics of skewed diagnostic data with both accuracy and precision. Although the Non-Parametric method attains the highest VUS across all scenarios, its practical application is constrained by sensitivity to sample size and data variability. In contrast, the Normal ROC model falls short in performance, producing unstable and less reliable estimates. Overall, the Log-Normal model emerges as a dependable and interpretable option, offering a balanced combination of theoretical rigor, computational efficiency, and diagnostic accuracy particularly well-suited for tri-class classification problems involving positively skewed and moderately sized datasets. Future research could focus on blending Parametric and Non-Parametric techniques to capitalize on the strengths of both methodologies.

Conflict of Interest

The authors declare no conflicts of interest

ACKNOWLEDGMENT

We are grateful to Amala R for her unwavering guidance and invaluable contributions to this research.

REFERENCES

1. Lin H, Zhou L, Peng H, Zhou XH. Selection and combination of biomarkers using ROC method for disease classification and prediction. Canadian Journal of Statistics. 2011 Jun;39(2):324-43.

2. Mayeux R. Biomarkers: potential uses and limitations. NeuroRx. 2004 Apr;1:182-8.

3. Krzanowski WJ, Hand DJ. ROC curves for continuous data. Chapman and Hall/CRC; 2009 May 21.

4. Bradley AP. The use of the area under the ROC curve in the evaluation of machine learning algorithms. Pattern recognition. 1997 Jul 1;30(7):1145-59.

5. Amala R, Pundir S. ROC Curve and AUC for A Left-Truncated Sample from Rayleigh Distribution. American Journal of Mathematical and Management Sciences. 2015 Apr 3;34(2):89-116.

6. Powell LA. Approximating variance of demographic parameters using the delta method: a reference for avian biologists. The Condor. 2007 Nov 1;109(4):949-54.

7. Amala R, Pundir S. Statistical inference on AUC from a bilognormal ROC model for continuous data. International Journal of Engineering Science and Innovative Technology. 2012;1(2):283-95.

8. Liu S, Zhu H, Yi K, Sun X, Xu W, Wang C. Fast and unbiased estimation of volume under ordered three-class ROC surface (VUS) with continuous or discrete measurements. IEEE Access. 2020 Jul 22;8:136206-22.

9. Nakas CT. Developments in ROC surface analysis and assessment of diagnostic markers in three-class classification problems. REVSTAT-Statistical Journal. 2014 Apr 1;12(1):43-65.

10. Qu Y, Cheng Y. Volume under the ROC surface for high-dimensional independent screening with ordinal competing risk outcomes. Lifetime Data Analysis. 2023 Oct;29(4):735-51.

11. Hanley JA, McNeil BJ. The meaning and use of the area under a receiver operating characteristic (ROC) curve. Radiology. 1982 Apr;143(1):29-36.

12. Dreiseitl S, Ohno-Machado L, Binder M. Comparing three-class diagnostic tests by three-way ROC analysis. Medical Decision Making. 2000 Jul;20(3):323-31.

13. Mossman D. Three-way rocs. Medical Decision Making. 1999 Jan;19(1):78-89.

14. Pundir S, Amala R. A study on the Bi-Rayleigh ROC model. Bonfring International Journal of Data Mining. 2012;2(2):42-7.

15. Heckerling PS. Parametric three-way receiver operating characteristic surface analysis using mathematica. Medical Decision Making. 2001 Oct;21(5):409-17.

16. Hughes G, Bhattacharya B. Symmetry properties of bi-normal and bi-gamma receiver operating characteristic curves are described by Kullback-Leibler divergences. Entropy. 2013 Apr 10;15(4):1342-56.